2014

Comparison and Generalization of R410A and R134a Distribution in the Microchannel Heat Exchanger with the Vertical Header

Yang Zou
University of Illinois at Urbana-Champaign, United States of America, yangzou1@illinois.edu

Predrag S. Hrnjak
pega@illinois.edu

Zou, Yang and Hrnjak, Predrag S., "Comparison and Generalization of R410A and R134a Distribution in the Microchannel Heat Exchanger with the Vertical Header" (2014). *International Refrigeration and Air Conditioning Conference.* Paper 1364.
http://docs.lib.purdue.edu/iracc/1364

Comparison and Generalization of R410A and R134a Distribution in the Microchannel Heat Exchanger with the Vertical Header

Yang ZOU[1,2], Pega HRNJAK[1,2]*

[1]University of Illinois at Urbana-Champaign, Department of Mechanical Science and Engineering,
Urbana, IL, USA

[2]Creative Thermal Solutions
Urbana, IL, USA
Contact Information (1-217-244-6377, yangzou1@illinois.edu, pega@illinois.edu)

* Corresponding Author

ABSTRACT

This paper explores the effects of fluid properties on two-phase flow in the vertical header and refrigerant distribution into horizontal branch tubes. R410A and R134a are used as the working fluid. Refrigerant enters into the header by five microchannel tubes in the bottom pass and exits through the five microchannel tubes in the top pass representing the flow in the outdoor microchannel heat exchanger of reversible systems under heat pump mode. The difference of fluid properties causes the flow pattern and refrigerant distribution results of R410A and R134a different between each other. Non-dimensional analysis shows that the inertia of R410A is higher than that of R134a. At low qualities, when the flow regime is churn, the higher inertia enables top tubes to receive more liquid so that the distribution of R410A is a little better than that of R134a. At high qualities, when it is likely semi-annular, the higher inertia causes more bottom tubes are bypassed by the liquid film of semi-annular flow. It results in worse R410A distribution than R134a, though more liquid reaches the top tubes for R410A. The coefficient of variation of refrigerant distribution is applied in this study to generalize the results of both R410A and R134a at various header geometries and inlet flow conditions. A distribution function is derived for predicting R410A and R134a distribution in future.

1. INTRODUCTION

The compactness and good heat transfer performance of the microchannel heat exchanger (MCHX) enables its broad use in both the residential and automotive air-conditioning system. However, refrigerant maldistribution in MCHX is a very important issue. It creates unwanted superheated region, where the heat transfer is lower than the two-phase region due to the lower heat transfer coefficient of superheated vapor and less temperature difference between refrigerant and air. Thus, the heat exchanger capacity is usually lower than the case with uniform distribution. Byun and Kim (2011) presented R410A maldistribution in a two-pass outdoor MCHX under heat pump (HP) mode caused the cooling capacity reduced up to 13.4% compared to the uniform distribution case. Zou et al. (2014) showed capacity degradation of 30% and 5% for R410A and R134a maldistribution in a two-pass outdoor MCHX under HP mode, respectively.

The knowledge to achieve good distribution is still limited, though it has been extensively studied. Fei and Hrnjak (2002), Vist and Pettersen (2004), Webb and Chung (2005), Bowers et al. (2006), and Hwang et al. (2007) studied the two-phase flow in the horizontal headers and refrigerant distribution into the vertical parallel tubes, which usually appeared in the indoor MCHX. Watanabe et al. (1995), Cho and Cho (2004), Lee (2009), Byun and Kim (2011), and Zou and Hrnjak (2013a, 2013b, 2014) investigated the refrigerant distribution in the inlet and/or intermediate vertical headers, which were commonly used in the outdoor MCHX. Maldistribution in the outdoor

MCHX was also very important when it was used as an evaporator in the heat pump mode. All of the above studies showed that maldistribution was a very complex problem that was affected by numerous parameters, such as header geometries and inlet flow conditions, etc. The flow regimes in the header, which was affected by the above parameters, had a strong influence on liquid distribution into the branch tubes in two-phase flow.

Zhang et al. (2003) and Kim et al. (2011) respectively compared the distribution of R134a with that of air-water mixture in a horizontal header (different geometries) with downward microchannel tubes. The fluid properties affected the two-phase flow velocities, which had a strong influence on refrigerant distribution. Because of the lower values of air density than R134, the velocity of air-water was higher. Thus, the rear tubes received more liquid for air-water while the front tubes got more liquid for R134a. To the authors' knowledge, no tests were done to compare the distribution of hydrocarbon refrigerants in the same geometry and the effects of fluid properties on two-phase flow in the vertical headers were not investigated. This paper is to clarify the effects of fluid properties on refrigerant distribution in the vertical header by comparing the experimental results of R134a and R410A.

2. EXPERIMENTAL METHOD

The test loop was constructed to study R410A or R134a distribution in the microchannel heat exchanger, as shown Figure 1. The subcooled liquid refrigerant was pumped into the inlet header. It was assumed that the single-phase subcooled liquid was distributed evenly into the microchannel tubes in the bottom pass, where the refrigerant was heated to the desired quality. The two-phase fluid entered into the test header and turned 90° to flow upward in the bottom part. In the upper part of the header, due to maldistribution, different amounts of liquid exited through the microchannel tubes in the top pass. In each exit tube, the refrigerant was heated again to provide equal superheat at the exit. The single phase superheated vapor was then brought to the condenser. Through the receiver and the subcooler, the subcooled liquid was returned to the pump.
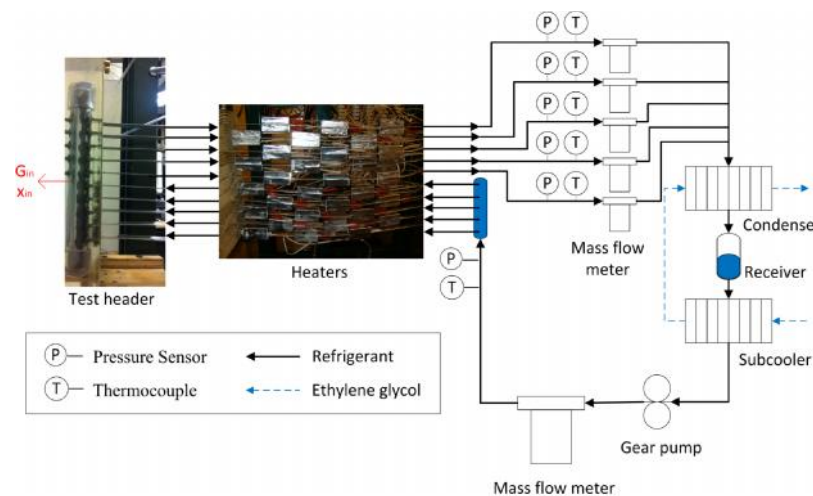

Figure 1: System schematics

The liquid mass flow rate in each exit tube was obtained by Equation (1).

$$m_{l,out,i} = m_{out,i}(1 - x_{out,i}) \text{ where } x_{out,i} = f(P_{header}, h_{out,i}) \qquad (1)$$

The pressure in the header P_{header} was estimated as the average of the measured subcooled and superheated pressures and the outlet enthalpy from the header (i.e., inlet to each exit tube) $h_{out,i}$ was calculated as in Equation (2).

$$h_{out,i} = h_{sup,i} - \frac{Q_{out,i}}{m_{out,i}} \text{ where } h_{sup,i} = f(P_{sup,}, T_{sup,i}) \qquad (2)$$

The liquid mass flow rate were generalized with coefficient of variation (Equation (3)) and liquid fraction (Equation (4)). Uniform distribution was described as $= 0$ and $LF_i = 0.2$. The worst distribution, for this case (five results), was when $= 2$. An uncertainty propagation analysis carried out in EES (2012). The uncertainty of measuring is within 4.5%. The uncertainty of liquid fraction is usually within 5%.

$$\dagger = \frac{1}{\overline{m}_l} \sqrt{\frac{1}{n} \sum_1^n (\dot{m}_{l,out,i} - \overline{m}_l)^2} \tag{3}$$

$$LF_i = \frac{\dot{m}_{l,out,i}}{\sum_i^n \dot{m}_{l,out,i}} \tag{4}$$

A high speed camera, Phantom v4.2, was used for visualizing the flow in the transparent header. The exposure time of the camera was 80 μsec. The framing rate was at 2000 frames per second. The resolution was 256x512 pixels. The transparent circular header, made of the PVC tube, had five inlet and five exit microchannel tubes protruded into the ½ depth of header's inner diameter. To examine the geometry effects, the number of tubes was doubled for both R410A and R134a and the tubes protrusion was increased to ¾ depth of header's inner diameter for R134a only. The geometries of the transparent header and aluminum microchannel tube are listed in Table 1. The test conditions are shown in Table 2. The inlet mass flux G_{in}, presented in Table 2, is defined by the smallest cross-section area in the header where tube protrusion is presented.

Table 1: Vertical header and microchannel tube geometries

Item	Data
Header geometry	
Inner diameter	15.44 mm
Header length	170 mm for 5+5 header; 300mm for 10+10 header
Tube pitch	13 mm
Tube protrusion	½ depth and ¾ depth of inner diameter
Microchannel geometry	
Shape	Rectangular
Number of ports	17
Length	0.54 mm
Width	0.5 mm
Hydraulic diameter	0.5 mm

Table 2: Test conditions

Item	Data
Saturation temperature	5 ºC for R410A; 10 ºC for R134a
Inlet quality	0.2 – 0.8
Inlet mass flow rate	2 – 6 g s^{-1} for 5+5 header; 2 – 12 g s^{-1} for 10+10 header
Inlet mass flux	21.80 – 129.00 kg m^{-2} s^{-1}

3. RESULTS AND DISCUSSION

The churn and semi-annular regimes are identified from the visualization for both R410A and R134a, as shown and listed in Figure 2 and Figure 3, where "C" denotes churn flow while "S" denotes semi-annular flow. The semi-annular flow is like annular flow, but due to the tubes protrusion, the annulus is not complete. The liquid distribution is better in churn flow because the opportunity of liquid supply to reach each branch tube is similar when liquid occupies most of the header, however, in the semi-annular flow, in only a small part of the header, liquid is easily available in front of the entrance to the tube. This small liquid region in semi-annular flow is bounded by the liquid film separation height h (called liquid separation) and the highest liquid level H (called liquid reach), as shown in

Figure 3. Figure 2 compares the two-phase flow and distribution of R410A and R134a at low qualities, i.e. $x_{in} = 0.2$, while Figure 3 illustrates the comparison at high qualities, i.e. $x_{in} = 0.8$. In each chart, the darkness of the bar color represents different branches (tubes), the pale being the lowest exit branch and the dark being the highest exit branch. At $x_{in} = 0.2$, the flow regime in the header is churn, so the mixing of vapor and liquid in the header is almost homogeneous. The maldistribution for both refrigerants is mainly caused by lack of enough momentum to supply liquid to the top tube, specifically at low inlet mass flow rate. The two-phase flow in the header and refrigerant distribution among the parallel tubes are similar for R410A and R134a. The distribution of R410A is a little better than R134a because the top tube gets a little more liquid. At $x_{in} = 0.8$, the flow regime is usually semi-annular. The difference between R410A and R134a is significant. At low mass flow rate such as 2.14 g s^{-1}, R134a distribution is worse than R410A because most liquid R134a is in the bottom tubes, however, at high mass flow rate such as 6.25 g s^{-1}, R410A distribution is worse than R134a due to the bottom tubes lack of liquid R410A. It is noticed that these differences are because of the similar reasoning: the liquid R410A flowes higher than liquid R134a at the same mass flow rate and quality conditions in the header. At low mass flow rate, such effect lifts R410A higher than R134a, resulting in better R410A distribution than R134a. At high mass flow rate, this effect makes the liquid film separation of R410A higher than that of R134a in semi-annular flow, so the bottom tubes have less opportunities to receive liquid for R410A, resulting in worse R410A distribution.
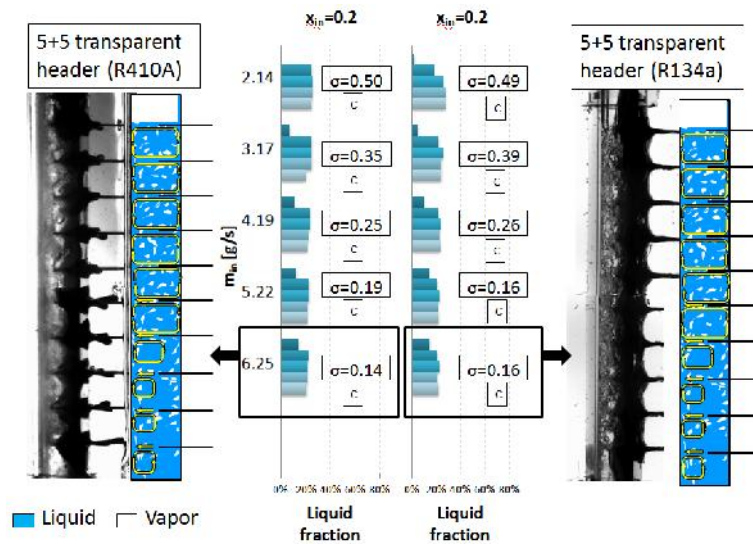

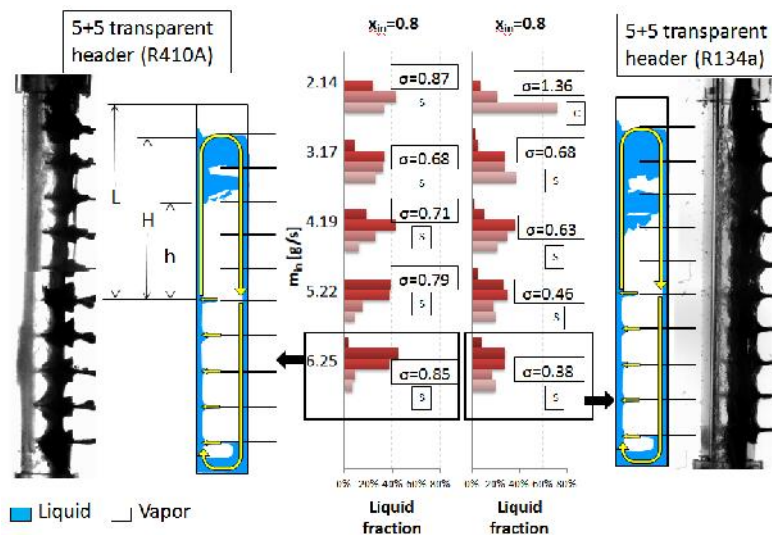**Figure 2:** R410A and R134a distribution comparison at low quality

Figure 3: R410A and R134a distribution comparison at high quality

The difference between R410A and R134 distribution may be explained by comparing the properties of these two refrigerants. Figure 4 presents the saturated vapor and liquid density and viscosity as well as the surface tension of R410A and R134a at the saturation temperature range from -10 °C to 15 °C. Table 3 presents quantitatively the properties difference at 10 °C. It is observed that R410A has lower surface tension, liquid density and viscosity but higher saturated vapor density and viscosity than R134a.
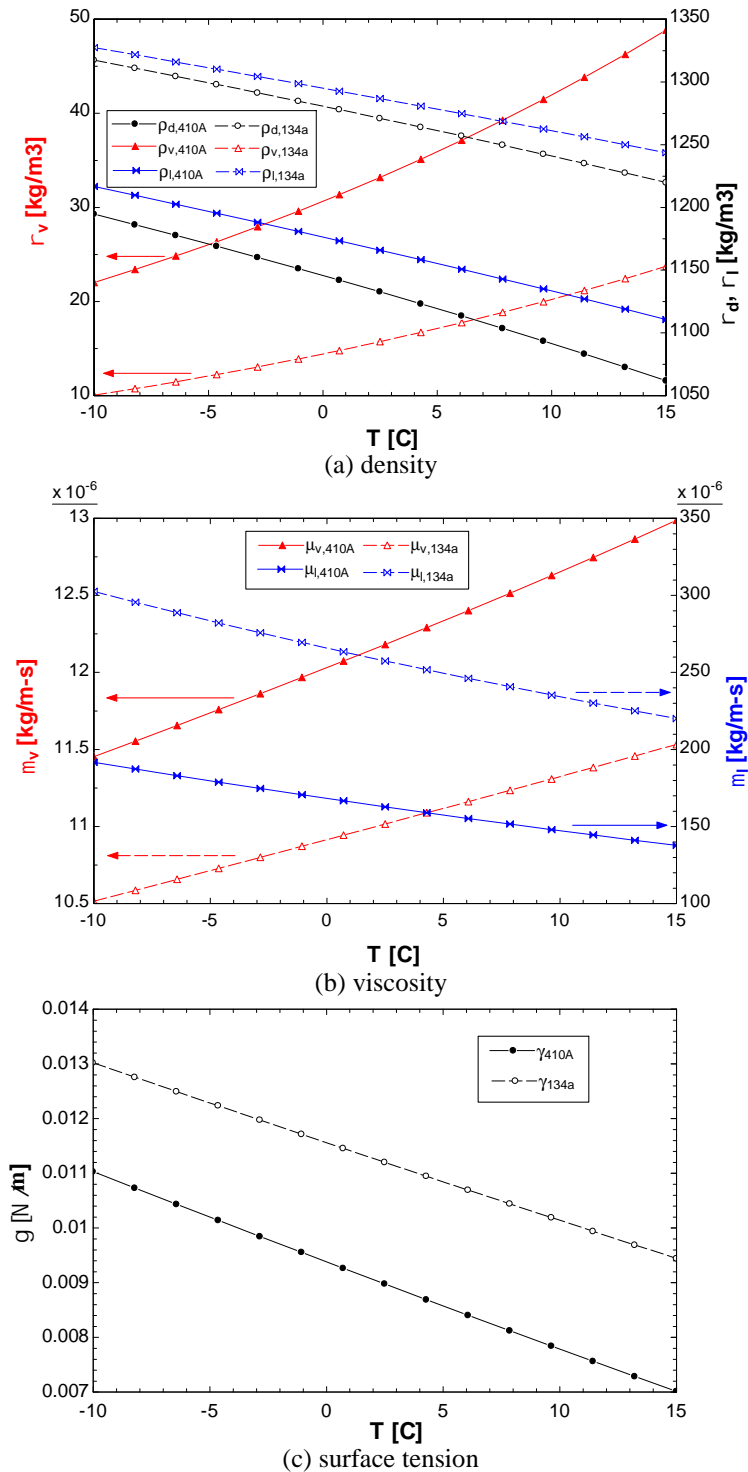

(a) density

(b) viscosity

(c) surface tension

Figure 4: Comparison of R410A and R134a properties

Table 3: R410A and R134a properties difference at 10 °C

| Properties	$\dfrac{y_{410A} - y_{134a}}{y_{134a}}$ %
Density difference $_d = _l - _v$	-12.07%
Liquid density $_l$	-10.15%
Vapor density $_v$	107.42%
Liquid viscosity μ_l	-37.11%
Vapor viscosity μ_v	11.75%
Surface tension	-23.22%

To explore the effects of the fluid properties, the non-dimensional analysis based on the Buckingham PI theorem is applied. It is found that the two-phase flow in the vertical header is governed by the Froude number (inertial force to gravity force), Reynolds number (inertial force to viscous force), and Weber number (inertial force to surface tension force). Because the interest of this study is where the liquid is, the liquid Froude number, liquid Reynolds number and liquid Weber number, defined in Equations (5) – (7), are examined. When the header geometries and the inlet flow conditions are the same for R410A and R134a, only the fluid properties affect the distribution. Since the liquid density, liquid and vapor density difference, liquid viscosity, and surface tension of R410A are lower than those of R134a, the liquid phase Froude number, Reynolds number, and Weber number of R410A are higher. Thus, the inertial force of liquid R410A is relatively more significant, so the liquid R410A can flow higher than liquid R134a. This effect cause the liquid reach and liquid separation of R410A is higher than those of R134a in Figure 5 and Figure 6, respectively. Since the distribution is better with the higher liquid reach (in both churn and semi-annular flow) but worse with the higher liquid separation height (in semi-annular flow), refrigerant distribution is the balance between these two effects. In semi-annular flow, the effect of liquid separation of R410A is more significant, resulting in worse R410A distribution than R134a at high inlet qualities and high inlet mass flow rate.

$$Fr_l = \frac{G(1-x)}{\sqrt{\cdots_l(\cdots_l - \cdots_v)gL}} \tag{5}$$

$$Re_l = G(1-x)\frac{D}{\tilde{\ }_l} \tag{6}$$

$$We_l = \cdots_l[\frac{G(1-x)}{\cdots_l}]^2\frac{D}{\mathsf{X}} = [G(1-x)]^2\frac{D}{\cdots_l\mathsf{X}} \tag{7}$$
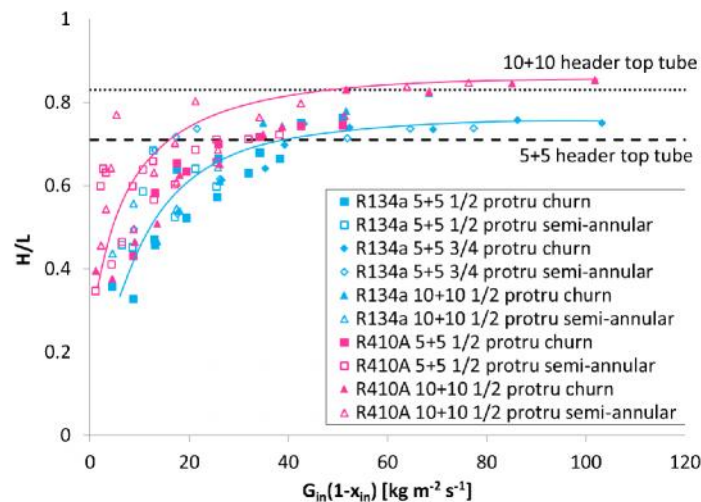
Figure 5: Liquid reach for R410A and R134a
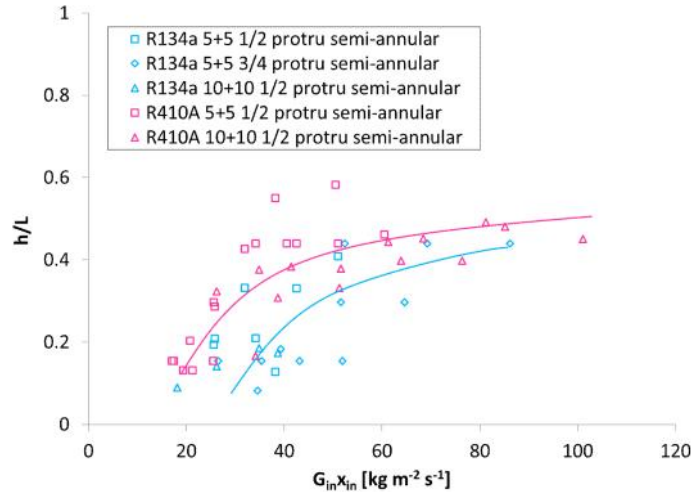
Figure 6: Liquid separation height for R410A and R134a

Hewitt and Roberts (1969) flow regime map for vertical tube was used to generalize the flow regimes of pure refrigerant in the vertical headers in Zou and Hrnjak (2013a & b). Since generalization of flow regimes could indicate refrigerant distribution, the same method is used to generalize the flow regimes of R134a and R410A, as shown in Figure 7. The superficial vapor momentum is a more important parameter than superficial liquid momentum. The transition line between churn flow and semi-annular flow is approximately at $_v j_v^2 = 10$. For good distribution, the header geometries and inlet flow conditions should be controlled so that the superficial vapor momentum is below 10 kg m^{-1}s^{-2}.
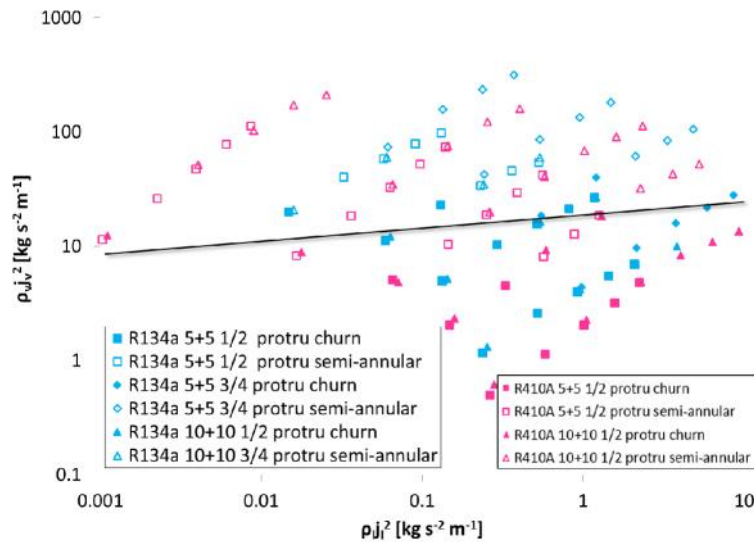
Figure 7: Flow regime map in the vertical header

The coefficient of variation, as an indicative of the overall liquid distribution in the intermediate header, are applied in this study to generalize the results by relating it to the liquid mass flux $G_l = G_{in}(1 - x_{in})$ in the middle of the header for both R410A and R134a with 5 or 10 tubes protruded into ½ or ¾ depth of internal diameter in each pass, as shown in Figure 8. The value of reduces as liquid mass flux increases, i.e. the distribution is better. The curve-fit correlation, as shown in Equation (8) is obtained through least square curve-fit method.

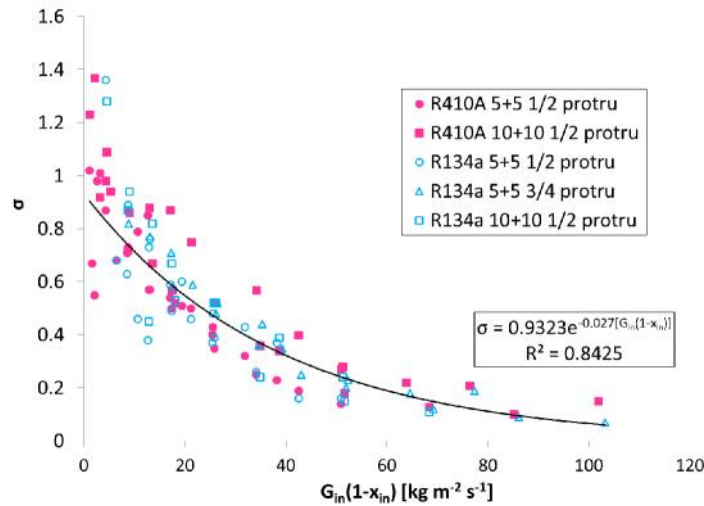$$† = 0.9323\exp[-0.027G_{in}(1 - x_{in})]$$

(8)

Figure 8: Coefficient of variation decreases as liquid mass flux increases

The distribution functions of Watanabe et al. (1995) and Byun and Kim (2011) relating liquid take-off ratio (ratio of liquid mass flow rate in the tube to liquid mass flow rate in the header immediately upstream) with vapor phase Reynolds number were proved to be good choice. The distribution function in this study is developed adopting the same parameters in the two-phase flow region in the header, i.e. below the liquid reach. In addition, the liquid take-off ratio is also related to the inlet quality. At any given inlet quality, the liquid take-off ratio reduces as Reynolds number increases at the same inlet quality, similar as the findings in Watanabe et al. (1995) and Byun and Kim (2011). The vapor phase Froude number is also introduced into the distribution function to consider the effects of fluid properties. The derived distribution function in Equation (9) is developed using least square curve-fit. The curve-fit in Figure 9 contains data of R410A and R134a with both 5+5 and 10+10 microchannel tubes protruded at ½ depth of header (D = 15 mm).

$$\Gamma = 1.75x_{in}^{1.206} Re_{v,M}^{-0.320} Fr_{v,M}^{-0.836} \tag{9}$$

where $\Gamma = \dfrac{\dot{m}_{l,out,i}}{\dot{m}_{l,M,i}}$, $Re_{v,M} = \dfrac{x_{M,i}\dot{m}_{M,i}D}{A\mu_v}$, and $Fr_{v,M} = \dfrac{x_{M,i}\dot{m}_{M,i}}{A\sqrt{\rho_v(\rho_l - \rho_v)gL}}$

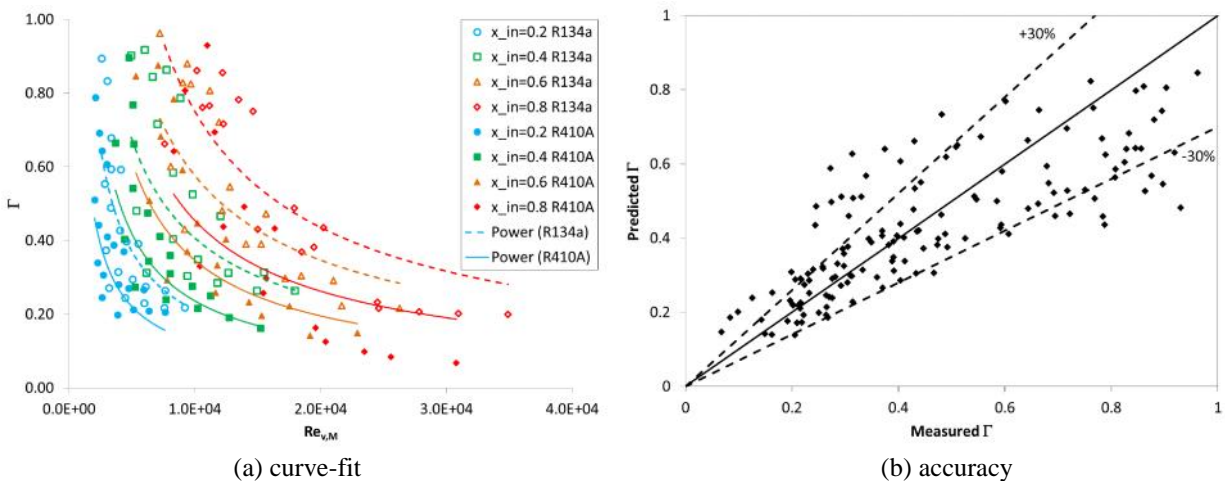(a) curve-fit   (b) accuracy

Figure 9: Distribution function

4. CONCLUSIONS

This study investigates R410A and R134a maldistribution in the vertical header and the impact on microchannel heat exchanger performance. The effects of fluid properties on the flow regime and refrigerant distribution are explored. At low qualities, since the flow regime is usually churn flow, the properties effects are not very significant. At high qualities, the difference between R410A and R134a properties causes R410A has higher liquid reach and liquid separation height than R134a. The bottom tubes suffer from the starvation of liquid refrigerant more significantly, though the liquid reach is higher, when R410A is the working fluid. Thus, R410A distribution is usually worse than R134a at high qualities. To generalize the results and predict refrigerant distribution in future, the coefficient of variation of refrigerant maldistribution for both refrigerants is related to the maximum liquid mass flux in the header, and a distribution function is obtained by relating the ratio of liquid mass flow rate in the tube to liquid mass flow rate in the header immediately upstream with the inlet quality and the vapor Reynolds number and Froude number in the header immediately upstream.

NOMENCLATURE

			Subscripts	
D	Header diameter	(m)	i	Branch number
Fr	Froude number	(-)	in	At the smallest
G	Mass flux	(kg m^{-2}s^{-1})		area in the middle
H	Liquid reach	(m)		of the header
h	Liquid separation height	(m)	l	Liquid
i	Enthalpy	(kJ kg^{-1})	out	Out of the header
j	Superficial velocity	(m s^{-1})	sup	Superheated
L	Length of the header exit part	(m)	sub	Subcooled
LF	Liquid fraction	(-)	v	vapor
m	Mass flow rate	(g s^{-1})		
n	Number of the outlet tubes	(-)		
Q	Power of the heaters	(kW)		
P	Pressure	(kPa)		
Re	Reynolds number	(-)		
T	Temperature	(K)		
We	Weber number (-)			
x	Quality	(-)		
Γ	Liquid take-off ratio	(-)		
γ	Surface tension	(N m^{-1})		
ρ	Density	(kg m^{-3})		
μ	Viscosity	(kg m^{-1}s^{-1})		
σ	Coefficient of variation	(-)		

REFERENCES

Bowers, C.D., Hrnjak, P.S., Newell, T.A., 2006. Two-phase refrigerant distribution in a micro-channel manifold. *Proc. 11th Int. Refrigeration Air Conditioning Conf. at Purdue*, R161.

Byun, H.W., Kim, N.H., 2011. Refrigerant distribution in a parallel flow heat exchanger having vertical headers and heated horizontal tubes. *Exp. Thermal Fluid Sci.* 35, 920-930.

Cho, H., Cho, K., 2004. Mass flow rate distribution and phase separation of R-22 in multi-microchannel tubes under adiabatic condition. *Microscale Thermophysical Eng.* 8 (2), 129-139.

Fei, P., Hrnjak, P.S., 2004. Adiabatic Developing Two-Phase Refrigerant Flow in Manifolds of Heat Exchangers. *Technical Report TR-225, Air Conditioning and Refrigeration Center, Univ. Illinois at Urbana-Champaign.*

Hewitt, G.F., Roberts, D.N., 1969. Studies of two-phase flow patterns by simultaneous X-ray and flash photography. *AERE-M 2159*, HMSO.

Hwang, Y., Jin, D.H., Radermacher, R., 2007. Refrigerant distribution in minichannel evaporator manifolds. *HVAC&R Res.* 13 (4), 543-555.

Kim, N.H., Kim, D.Y., Byun, H.W., 2011. Effect of inlet configuration on the refrigerant distribution in a parallel flow minichannel heat exchanger. *Int. J. Refrigeration.* 34, 1209-1221.

Lee, J.K., 2009. Two-phase flow behavior inside a header connected to multiple parallel channels. *Exp. Thermal Fluid Sci.* 33, 195-202.

Vist, S., Pettersen, J., 2004. Two-phase flow distribution in compact heat exchanger manifolds. *Exp. Thermal Fluid Sci.* 28, 209-215.

Watanabe, M., Katsuta, M., Nagata, K., 1995. General characteristics of two-phase flow distribution in a multipass tube. *Heat Transfer-Japanese Res.* 24, 32-44.

Webb, R.L., Chung, K., 2005. Two-phase flow distribution to tubes of parallel flow air-cooled heat exchangers. *Heat Transfer Eng.* 26 (4), 3-18.

Zhang, Q.M., Hrnjak, P.S., Newell, T.A., 2003. An experimental investigation of R134a flow distribution in horizontal microchannel manifolds. Technical Report TR-223. *Air Conditioning and Refrigeration Center, Univ. Illinois at Urbana-Champaign.*

Zou, Y., Hrnjak, P.S., 2013a. Experiment and visualization on R134a upward flow in the vertical header of microchannel heat exchanger and its effect on distribution. *Int. J. Heat and Mass Trans.* 62, 124-134.

Zou, Y., Hrnjak, P.S., 2013b. Refrigerant distribution in the vertical header of the microchannel heat exchanger - measurement and visualization of R410A flow. *Int. J. Refrigeration.* 36, 2196-2208.

Zou, Y., Hrnjak, P.S., 2014. Effect of oil on R134a distribution in the microchannel heat exchanger with vertical header. Int. J. Refrigeration. *Int. J. Refrigeration.* 40, 201-210.

Zou, Y., Tuo, H., Hrnjak, P.S., 2014. Modeling refrigerant maldistribution in microchannel heat exchangers with vertical headers based on experimentally developed distribution results. *Appl. Thermal Eng.* 64, 172-181.

ACKNOWLEDGEMENT